AIP | Applied Physics Letters

Flexoelectric strain gradient detection using Ba0.64Sr0.36TiO3 for sensing

Wenbin Huang, Xiang Yan, Seol Ryung Kwon, Shujun Zhang, Fuh-Gwo Yuan et al.

Citation: Appl. Phys. Lett. **101**, 252903 (2012); doi: 10.1063/1.4772803
View online: http://dx.doi.org/10.1063/1.4772803
View Table of Contents: http://apl.aip.org/resource/1/APPLAB/v101/i25
Published by the American Institute of Physics.

Related Articles

Effect of Ni-substitution on glass forming ability, mechanical, and magnetic properties of FeBNbY bulk metallic glasses
J. Appl. Phys. 113, 013505 (2013)

Pre-curving analysis of an opening crack in a magnetoelectroelastic strip under in-plane impact loadings
J. Appl. Phys. 112, 124911 (2012)

Fatigue properties of atomic-layer-deposited alumina ultra-barriers and their implications for the reliability of flexible organic electronics
Appl. Phys. Lett. 101, 251901 (2012)

Kinetics of hardness evolution during annealing of gamma-irradiated polycarbonate
J. Appl. Phys. 112, 113509 (2012)

Piezoresistance behaviors of ultra-strained SiC nanowires
Appl. Phys. Lett. 101, 233109 (2012)

Additional information on Appl. Phys. Lett.

Journal Homepage: http://apl.aip.org/
Journal Information: http://apl.aip.org/about/about_the_journal
Top downloads: http://apl.aip.org/features/most_downloaded
Information for Authors: http://apl.aip.org/authors

ADVERTISEMENT

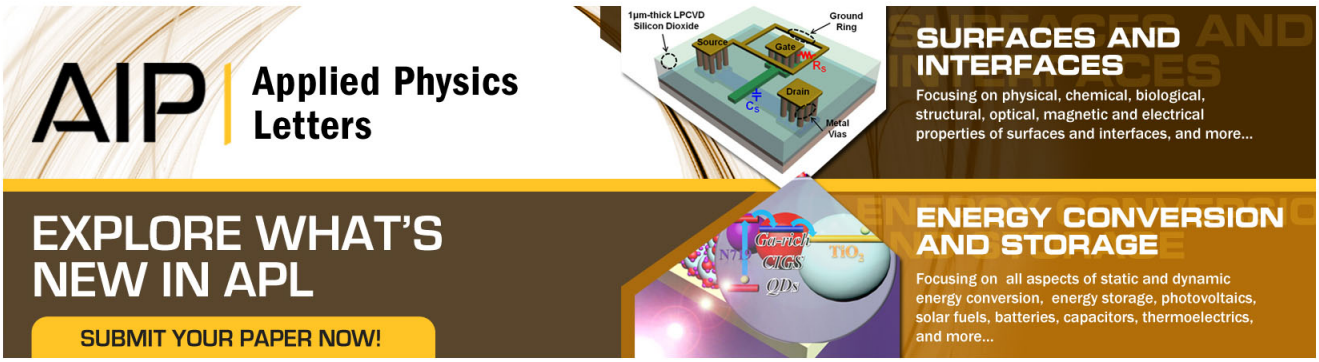

Flexoelectric strain gradient detection using $Ba_{0.64}Sr_{0.36}TiO_3$ for sensing

Wenbin Huang,[1] Xiang Yan,[1] Seol Ryung Kwon,[1] Shujun Zhang,[2] Fuh-Gwo Yuan,[1] and Xiaoning Jiang[1,a)]
[1]*Department of Mechanical and Aerospace Engineering, North Carolina State University, Raleigh, North Carolina 27695, USA*
[2]*Materials Research Institute, Pennsylvania State University, University Park, Pennsylvania 16802, USA*

(Received 10 September 2012; accepted 5 December 2012; published online 19 December 2012)

Strain gradient sensing offers an alternative avenue for *in-situ* monitoring of onset and growth of cracks in structural health monitoring, where the strain gradient is the most sensitive measurand. In this study, flexoelectric strain gradient sensing structures using $Ba_{0.64}Sr_{0.36}TiO_3$ (BST) were attached on the proximity of an open hole in an aluminum plate, to monitor strain gradient variations of the specimen under a uniaxial dynamic load. Charge outputs of the BST micro-bars showed good linearity with the average strain gradients, with a sensitivity of 88 pC m, which is in good agreement with the theoretical estimation by assuming a 30 μm bonding thickness. © *2012 American Institute of Physics*. [http://dx.doi.org/10.1063/1.4772803]

Fatigue cracks are the most common form of damage in metallic structures, demonstrated in various inspections as well as in major aircraft fatigue tests.[1] 70% of the damage discovered resulted from such cracks. The holes were the second most common fatigue damage initiation site that leads to the major accident of aircraft between 1947 and 1983.[2] Developing sensing method for *in-situ* monitoring of the onset and growth of cracks at the early stage, especially near the severe strain gradient fastener areas is of growing interest. At present, existing sensing technology (e.g., strain gauges, accelerometers, linear voltage displacement transducers) is not effective for monitoring damage because of its limited sensitivity, bandwidth, and accessibility to the hidden localized areas, let alone damage initiation and progression.[3] Recent research progress on flexoelectricity (FE) suggests a new type of sensors—strain gradient sensors (SGS), which enable highly sensitive detection of strain gradient—the most sensitive measurand near the localized damage location.

In a piezoelectric material such as lead zirconate titanate (PZT), an applied uniform strain can generate electric polarization (or voltage for open circuit) or vice versa. This direct/converse piezoelectric effect (PE) is a well-recognized and much exploited in a broad sensors and actuators applications. In crystallography, this PE phenomenon only exists in non-centrosymmetirc crystal systems (20 out of 32 point groups). Non-uniform strain or strain gradient can, however, locally breaks inversion symmetry and induces voltage even in centrosymmetirc crystals. This phenomenon is termed FE. The FE exists in all dielectric solids. This opens up much broader choice of materials including lead and no-lead dielectrics with preferable properties.[4] In 1964, Kogan[5] first discussed the electric polarization induced in a centric crystal by inhomogeneous deformation and proposed the electromechanical coupling relationships of FE which can be described as

$$P_l = \mu_{ijkl}\frac{\partial \varepsilon_{ij}}{\partial x_k}, \tag{1}$$

where P_l is the flexoelectric polarization, μ_{ijkl} is the flexoelectric coefficient, ε_{ij} is the elastic strain, and x_k is the position coordinate. μ_{ijkl} is a fourth-rank polar tensor and therefore has nonzero components μ_{1111}, μ_{1122}, μ_{2323}, or in matrix notation μ_{11}, μ_{12}, μ_{44} in a cubic crystal. Kogan also suggested an estimation of the order of magnitude of the flexoelectric coefficient as $\mu_{ijkl} \approx e/a$, where e is the charge of the electron and a is the atomic dimension of the unit cell of the dielectric. Phenomenological arguments indicated that this value for normal dielectrics should be multiplied by the relative permittivity for the case of high permittivity materials including ferroelectrics.[6] Recent experimental research work done by Ma and Cross[7] confirmed the theory and showed that flexoelectric coefficient in the ferroelectric materials are many orders of magnitude higher (10^{-6}–10^{-4} C/m) than that in simple dielectrics ($\sim 10^{-10}$ C/m).

The $Ba_xSr_{1-x}TiO_3$ (BST) ceramic presented the highest flexoelectric coefficients among all reported ferroelectric materials up to now.[8] In this study, BST with the composition of Ba:Sr = 64%:36% was lab-prepared using a conventional solid state processing method. The Young's modulus of the BST is 152 GPa and Poisson ratio is 0.33. The Curie temperature of the prepared BST samples is about 18 °C and the dielectric constant at room temperature is about 14 000. By using the cantilever beam based direct measurement introduced in another paper,[9] the transverse flexoelectric coefficient μ_{12} was measured to be about 45 μC/m. In order to characterize the strain gradient sensing, a BST micro-bar (5 mm × 1 mm × 300 μm) obtained by lapping and polishing was mounted near the central hole in an aluminum plate subjected to a uniaxial tension. Large strain gradient exists nearby the hole due to the large stress concentration.[10] Assuming that the strain gradient transmitted to the attached BST micro-bar is in plane, the induced charge should be collected at the electrodes with the configuration shown in Figure 1. Coaxial wires were bonded to the sidewall

a)Author to whom correspondence should be addressed. Electronic mail: xjiang5@ncsu.edu.

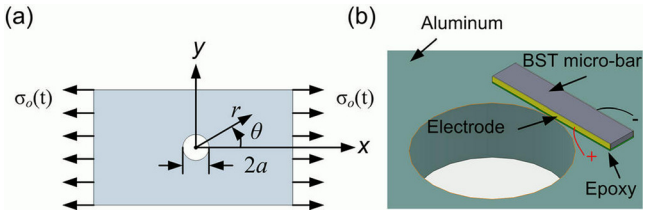

FIG. 1. Circular hole in a plate subjected to uniaxial tension.

electrodes using silver paste to eliminate the external noise. The positive wire connected the inner side relative to the central hole, while the ground wire to the outer side. Epoxy adhesive (Hysol EA 9359.3) was used to bond the BST micro-bar to the aluminum substrate. A pressure of 0.2 MPa was applied to ensure the flatness of the epoxy layer, which was measured to be about 50 μm. The epoxy layer is also essential for insulating the sidewall electrodes from the metal substrate. The shear strength of the epoxy at room temperature is 1.03 GPa. The dimension of the aluminum substrate is 200 mm× 38 mm× 3.2 mm.

The stress distribution near the open hole in polar coordinates under plane stress can be presented as[10]

$$\sigma_r/\sigma_o = \frac{1}{2}\left[\left(1-\frac{a^2}{r^2}\right)+\left(1+\frac{3a^4}{r^4}-\frac{4a^2}{r^2}\right)\cos 2\theta\right],$$
$$\sigma_\theta/\sigma_o = \frac{1}{2}\left[\left(1+\frac{a^2}{r^2}\right)-\left(1+\frac{3a^4}{r^4}\right)\cos 2\theta\right], \quad (2)$$

where a is the hole radius, σ_o is the nominal stress induced by the uniaxial load at the location far away from the hole, r and θ are the coordinates of polar coordinate system, and σ_r and σ_θ are the stress in radial and tangential directions, respectively. The stress distribution in Cartesian coordinates can be obtained through coordinate transformation and the corresponding strain components can be derived as

$$\varepsilon_x = \frac{1}{E}(\sigma_x - \nu\sigma_y),$$
$$\varepsilon_y = \frac{1}{E}(\sigma_y - \nu\sigma_x), \quad (3)$$

where v is the Poisson ratio, E is the Young's modulus, ε_x, σ_x and ε_y, σ_y are the strain and stress in x and y directions, respectively. The aluminum substrate has the Young's modulus of 73 GPa and Poisson ratio of 0.3. Strain gradient tensors can then be obtained by numerical differentiation of the strain tensors. Normalized strain and strain gradient distribution near the central hole with the radius of 2.5 mm under the nominal tension stress of 1 MPa are shown in Figure 2.

Since a finite thickness adhesive layer bonds between the BST micro-bar and the aluminum substrate, the strain or strain gradient in the substrate cannot be fully transmitted into the BST bar, known as the shear lag effect.[11] The derivation of the correction factor to account for shear lag effects was presented by Crawley and de Luis.[11] Consider a sensor with length l_c, width b_c, and thickness t_c and Young's modulus Y_c bonded onto the beam with length l_b, width b_b, and thickness t_b. Let the thickness of the bond layer be t_s. Sensed relative strain $\zeta(\varepsilon_c/\varepsilon_b)$ has the solution of[11]

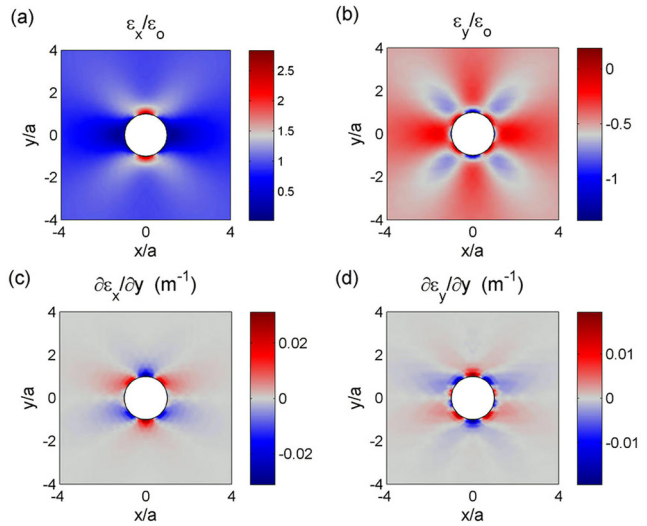

FIG. 2. Strain and strain gradient distribution near the central hole in a aluminum plate (radius = 2.5 mm) with 1 MPa nominal tension stress. Distribution of (a) normalized ε_x, (b) normalized ε_y, (c) $\partial\varepsilon_x/\partial y$, and (d) $\partial\varepsilon_y/\partial y$.

$$\zeta = \frac{\cosh \Gamma l_c - 1}{\sinh \Gamma l_c}\sinh \Gamma x - \cosh \Gamma x + 1\,, \quad (4)$$

where G is the shear modulus of the bond layer material and Γ is defined as

$$\Gamma^2 = \frac{G}{Y_c t_c t_s} + \frac{4Gb_c}{Y_b b_b t_b t_s}\,. \quad (5)$$

Substituting the dimensions to the equations, the correction factors of ε_x and ε_y can be calculated individually and plotted in Figure 3. It can be observed that the maximum strain transmission happens at the center point of the sensor, while there is no strain transmitted to the sensor at the boundary. ε_x at the center of the sensor was found to be on the order of 65% of the value in the substrate, while ε_y degrade greatly due to the short width of the sensor.

With the transmitted strain gradient, the generated polarization in the BST micro-bar, induced by FE effect, can be written as

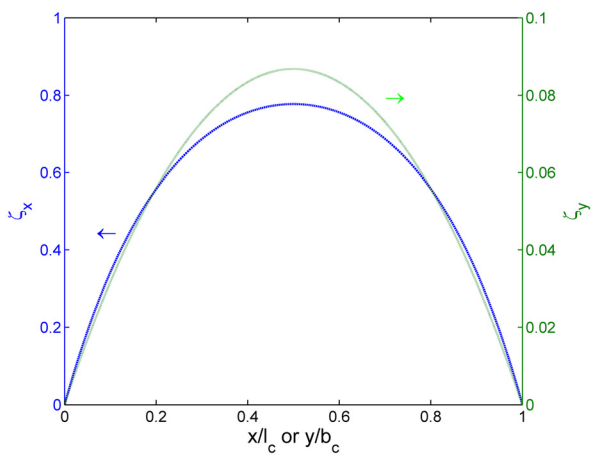

FIG. 3. Shear lag effects along sensor length and width.

$$P_y = \mu_{12}\frac{\partial \varepsilon_{cx}}{\partial y} + \mu_{11}\frac{\partial \varepsilon_{cy}}{\partial y} = \mu_{12}\frac{\partial(\zeta_x \varepsilon_{bx})}{\partial y} + \mu_{11}\frac{\partial(\zeta_y \varepsilon_{by})}{\partial y}, \quad (6)$$

where ε_{cx} and ε_{cy} are strain components in the BST micro-bar, ε_{bx} and ε_{by} are the strain components in the aluminum substrates, and ζ_x and ζ_y are the correction factors in x and y directions, respectively. The averaged polarization is given by

$$\overline{P}_y = \mu_{12}\frac{1}{l_c}\int_0^{l_c}\frac{\varepsilon_{cx}|_{b_c} - \varepsilon_{cx}|_0}{b_c}dx + \mu_{11}\frac{1}{l_c}\int_0^{l_c}\frac{\varepsilon_{cy}|_{b_c} - \varepsilon_{cy}|_0}{b_c}dx. \quad (7)$$

By multiplying the correction factor with strain gradient distribution in the aluminum, strain gradient distribution in the sensor can be obtained. The first part of the right hand side of Eq. (7), which arises from the average transverse strain gradient $\overline{\varepsilon}_{cx,y}$, is about $0.0036\,\mathrm{m}^{-1}$ under the nominal stress of 1 MPa, and the average transverse strain gradient $\overline{\varepsilon}_{cx,y}$ without considering the shear lag effect is about $0.0055\,\mathrm{m}^{-1}$. However, the second part of it, which is associated with the average longitudinal strain gradient $\overline{\varepsilon_{cy,y}}$, is zero due to boundary condition of the shear lag effect. Hence the charge output (Q) can be given by

$$Q = l_c t_c \overline{P}_y = l_c t_c \mu_{12} \overline{\varepsilon}_{cx,y}. \quad (8)$$

Experiment was conducted on a hydraulic tester (Instron 1331). The charge output from the BST micro-bar was monitored using a charge amplifier, with the stress swept from 1 MPa to 5 MPa at 2 Hz. Figure 4 shows the real time charge outputs of the BST micro-bar under a sinusoidal nominal stress with the peak-peak value of 3 MPa, where it can be observed that the charge output is out-of-phase with the load. This is because that the strain decreases along the radial direction under tension stress, causing the strain gradient in the BST micro-bar pointing from its outer side to its inner side relative to the hole center, which is opposite to the wire connection.

Figure 5 illustrates the relationship between the flexoelectric charge output of the BST micro-bar with the average strain gradient of the substrate. The average strain gradient under particular nominal stress was estimated through the theoretical calculation, including the shear lag effect from a 50 μm thick bonding layer. The slopes of the polarization versus average strain gradient curves can be defined as the sensitivity of SGS, with the unit of C m. The charge outputs of the BST micro-bar show good linearity with the average strain gradients. The sensitivity of the BST micro-bar was found to be about 88 pC m, while the sensitivity obtained from theoretical calculation is about 68 pC m.

The slight discrepancy between the sensor outputs with the theoretical estimation may be due to several sources. First, the thickness and uniformity of the adhesive bonding layer play an important role in the strain gradient transmission. Under 1 MPa nominal stress, with the thickness of the bonding layer decreasing from 60 μm to 20 μm, the average strain gradient transmitted to the BST micro-bar increases from $0.003\,\mathrm{m}^{-1}$ to $0.005\,\mathrm{m}^{-1}$, accounting for 67% difference. Thus, the actual sensitivity of the BST micro-bar SGS should be higher than the original expectation, as we assumed the thickness of the adhesive layer to be 50 μm during theoretical analysis, where the experimental results will be in good agreement with the theoretical evaluation if assuming a bonding thickness of 30 μm. Second, deflection of the BST micro-bar from the tangency of the hole circumference will lead to inconsistence between the theoretical calculations and the real measurand. Besides, the non-ideal circular degree of the central hole may induce a disagreement between the theoretical strain model with the real strain distribution. Hence in order to eliminate the discrepancy between experimental output of BST micro-bar with theoretical analysis, future work will involve more precise control of the bonding layer thickness and uniformity, as well as better alignment of the BST micro-bar with the hole or other damage locations.

Different from the direct strain gradient sensing using BST micro-bars, fiber-optic bragg grating (FBG) sensors have been widely applied to monitor the strain distribution with resolution in the range of $\mu\varepsilon$, and through which strain gradient can be indirectly measured.[12,13] Considering that the spatial resolution of 1 mm for FBG sensing, the

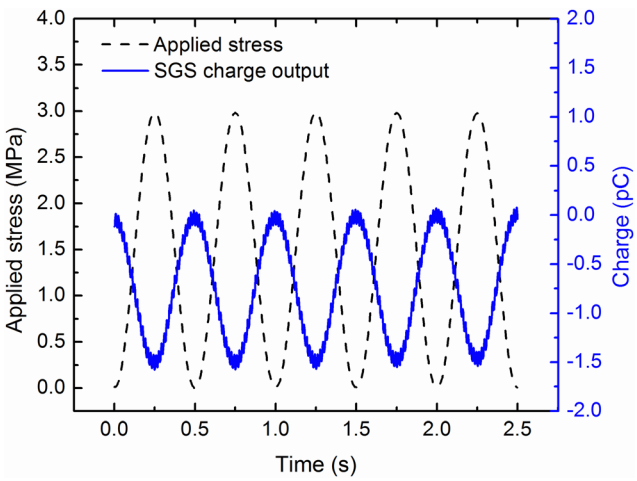

FIG. 4. Real time charge outputs from a BST micro-bar.

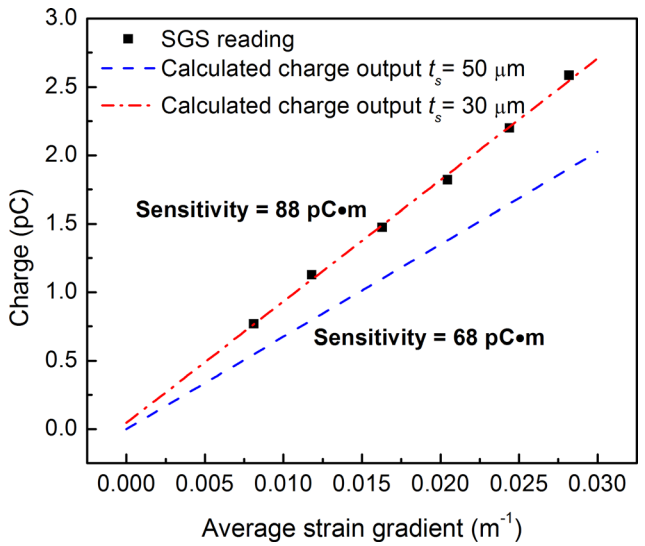

FIG. 5. Relationships between the theoretically estimated and measured charge outputs with average strain gradients of the BST micro-bar SGS.

calculated strain gradient measurement resolution can be about $0.001\,m^{-1}$, which is similar to that of SGS sensor assuming a charge measurement resolution of 0.1 pC and SGS sensitivity of 88 pC m. Distributed strain gauges and piezoelectric sensors are the common counterparts of FBG sensors in structural strain monitoring and hence could also be used for indirect measurement of strain gradient.[14,15] However, relatively large sizes of distributed strain gauges, piezoelectric sensors, and FBG sensors hinder the precise measurement of localized strain gradient, which exists around micro-cracks in structures.

In summary, a type of flexoelectric sensor based on BST micro-bar to capture the strain gradient was demonstrated for the detection of the most sensitive measurand near the localized damage location. Experimental charge outputs of the BST micro-bar SGS showed good linearity with the average strain gradients with a sensitivity of 88 pC m. The results demonstrate that the flexoelectric sensing technique is promising for structural health monitoring.

This material is based upon work supported by, or in part by, the U.S. Army Research Laboratory and the U. S. Army Research Office under Contract/Grant No. W911NF-11-1-0516; and in part by National Science Foundation under Grant No. CMMI-1068345.

[1]C. Boller, Int. J. Syst. Sci. **31**(11), 1333 (2000).
[2]G. S. Campbell and R. Lahey, Int. J. Fatigue **6**(1), 25 (1984).
[3]C. R. Farrar and K. Worden, Philos. Trans. R. Soc. London, Ser. A **365**(1851), 303 (2007).
[4]A. K. Tagantsev, V. Meunier, and P. Sharma, MRS Bull. **34**(9), 643 (2009).
[5]S. M. Kogan, Sov. Phys. Solid State **5**(10), 2069 (1964).
[6]A. K. Tagantsev, Phys. Rev. B **34**(8), 5883 (1986).
[7]L. E. Cross, J. Mater. Sci. **41**(1), 53 (2006).
[8]W. H. Ma and L. E. Cross, Appl. Phys. Lett. **81**(18), 3440 (2002).
[9]W. B. Huang, K. Kim, S. J. Zhang, F. G. Yuan, and X. N. Jiang, Phys. Status Solidi (RRL) **5**(9), 350 (2011).
[10]A. E. Armenàkas, *Advanced Mechanics of Materials and Applied Elasticity* (CRC, 2006).
[11]E. F. Crawley and J. De Luis, AIAA J. **25**(10), 1373 (1987).
[12]M. LeBlanc, S. Y. Huang, M. Ohn, R. M. Measures, A. Guemes, and A. Othonos, Opt. Lett. **21**(17), 1405 (1996).
[13]G. Zhou and L. M. Sim, Smart Mater. Struct. **11**(6), 925 (2002).
[14]B. F. Spencer, M. E. Ruiz-Sandoval, and N. Kurata, Struct. Control Health Monit. **11**(4), 349 (2004).
[15]S. F. Yuan, D. K. Liang, L. H. Shi, X. Zhao, J. Wu, G. Li, and L. Qiu, J. Intell. Mater. Syst. Struct. **19**(3), 373 (2008).